Three-Dimensional Structure of Bacterial Luciferase from *Vibrio harveyi* at 2.4 Å Resolution[†,‡]

Andrew J. Fisher,[§] Frank M. Raushel,[∥] Thomas O. Baldwin,[⊥] and Ivan Rayment*[,§]

Department of Biochemistry and Institute for Enzyme Research, University of Wisconsin, 1710 University Avenue, Madison, Wisconsin 53705, and Department of Chemistry and Department of Biochemistry and Biophysics and Center for Macromolecular Design, Texas A&M University, College Station, Texas 77843

Received March 13, 1995; Revised Manuscript Received March 29, 1995[⊗]

ABSTRACT: Luciferases are a class of enzymes that generate light in the visible spectrum. Luciferase from luminous marine bacteria is an alpha−beta heterodimer monooxygenase that catalyzes the oxidation of $FMNH_2$ and a long-chain aliphatic aldehyde. The X-ray crystal structure of bacterial luciferase from *Vibrio harveyi* has been determined to 2.4 Å resolution. The structure was solved by a combination of multiple isomorphous replacement and molecular averaging between the two heterodimers in the asymmetric unit. Each subunit folds into a $(\beta/\alpha)_8$ barrel motif, and dimerization is mediated through a parallel four-helix bundle centered on a pseudo 2-fold axis that relates the structurally similar subunits. The vicinity of the active site has been identified on the alpha subunit by correlations with similar protein motifs and previous biochemical studies. The structure presented here represents the first molecular model of a bioluminescent enzyme.

The generation of light by living organisms such as fireflies, glowworms, luminescent fish, or simple bacteria has been a source of fascination throughout the ages. Part of the interest in bioluminescence, dating from the early experiments of Robert Boyle (Boyle, 1668), is that intense light emission is not accompanied by high temperatures. Surprisingly, the chemistry behind these luminescent processes is quite variable. However, all the bioluminescent reactions are oxidative processes that convert a substrate to an electronically excited product, which emits a photon of visible light upon conversion to the ground state. The substrate that luciferase activates is generally referred to as luciferin, although the different bioluminescent reactions use different oxidizable substrates. These reactions are catalyzed by luciferases, an evolutionarily diverse group of enzymes that share only the feature of generation of an excited-state product resulting in bioluminescence. Until now, little has been known of the structural framework of any of the enzymes that mediate these bioluminescent reactions.

The luciferase of luminous bacteria, which has no evolutionary relationship with any other luciferase studied so far, is a flavin monooxygenase [for review see Baldwin and Ziegler (1992)]. The enzyme catalyzes the reaction of $FMNH_2$, O_2, and a long-chain aliphatic aldehyde to yield FMN, the aliphatic carboxylic acid, and blue-green light.

$$FMNH_2 + O_2 + RCHO \rightarrow FMN + RCOOH + H_2O + h\nu \quad (\lambda_{max} \approx 490\ nm)$$

Luciferase from all bacterial species studied to date consists of two subunits, alpha and beta, with molecular masses of approximately 40 and 35 kDa, respectively. Bacterial luciferase is an uncommon flavoprotein in that it employs reduced flavin as a substrate rather than a tightly bound cofactor. One reduced flavin molecule binds to the luciferase dimer (Becvar & Hastings, 1975; Meighen & Hastings, 1971). Molecular oxygen reacts with carbon 4a of the bound flavin to form an activated hydroperoxyflavin species (Hastings et al., 1973). The enzyme-bound C4a-hydroperoxyflavin intermediate then binds a long-chain aldehyde. The flavin intermediate oxidizes the aldehyde to the carboxylic acid and emits a quantum of light with an overall quantum efficiency of roughly 10%. The active site appears to reside on the alpha subunit (Baldwin & Ziegler, 1992; Cline & Hastings, 1972). The role of the beta subunit is not yet understood, but beta is essential for a high quantum yield. The two subunits are likely the result of gene duplication through the course of evolution (Baldwin et al., 1979). Amino acid sequence alignment of the two subunits reveals that they share 32% sequence identity, and the alpha subunit contains 29 additional amino acids inserted at residue 259 of the beta subunit (Cohn et al., 1985; Johnston et al., 1986). Separate alpha and beta subunits, purified from recombinant *Escherichia coli* independently carrying the *lux*A or *lux*B genes, do support a bioluminescent reaction, but the quantum efficiency is 6 orders of magnitude below that of the heterodimer (Waddle & Baldwin, 1991). However, the active dimer fails to assemble when the purified alpha and beta subunits are combined (Sinclair et al., 1993; Waddle et al., 1987). Functional dimers can assemble upon renaturation of the unfolded individual subunits (Baldwin et al., 1993). Much work has been done toward understanding the function of this intriguing enzyme. Here we report

[†] This research was supported in part by grants from the NIH (GM33894 to F.M.R., AR35186 to I.R., and Fellowship AR08304 to A.J.F.), the Robert A. Welch Foundation (A-840 to F.M.R. and A-865 to T.O.B.), and the Office of Naval Research (N00014-91-J-4097 and N00014-92-J-1900 to T.O.B.).

[‡] The coordinates have been deposited in the Brookhaven Protein Data Bank (file name 1BRL).

* To whom correspondence should be addressed.

[§] Department of Biochemistry and Institute for Enzyme Research, University of Wisconsin.

[∥] Department of Chemistry, Texas A&M University.

[⊥] Department of Biochemistry and Biophysics and Center for Macromolecular Design, Texas A&M University.

[⊗] Abstract published in *Advance ACS Abstracts,* May 1, 1995.

0006-2960/95/0434-6581$09.00/0

Table 1: Bacterial Luciferase Structure Determination Data Statistics

	compound				
	native CHESS	native HI-STAR[b]	TMLA[a] HI-STAR[b]	$K_2Pt(CN)_6$ HI-STAR[b]	$KAu(CN)_2$ HI-STAR[b]
resolution (Å)	2.4	2.9	2.9	2.9	2.9
measurements	290488	139224	120995	72240	62633
unique reflections	74342	44220	41146	34783	25791
percentage data	92	97	90	76	56
R_{merge}[c]	11.5	7.8	7.7	7.3	10.1
R_{iso}[d]			13.0	18.4	31.5
R_{Cullis}[e]			0.64	0.72	0.69
phasing power[f]			1.0	0.67	0.88
soaking time (days)			15	4	1
concn (mM)			5.0	0.5	0.75
no. of sites			10	6	8

[a] TMLA = trimethyllead acetate. [b] HI-STAR = Siemens HI-STAR dual-detector system. [c] $R_{merge} = [\sum_h \sum_i |I_h - I_{hi}| / \sum_h \sum_i I_{hi}] \times 100$, where I_h is the mean of the I_{hi} observations of reflection h. [d] $R_{iso} = \sum ||F_{PH}| - |F_P|| / \sum |F_{PH}| \times 100$. [e] $R_{Cullis} = \sum ||F_{PH(obs)} \pm F_{P(obs)}| - F_{H(calc)}| / \sum ||F_{PH(obs)}| \pm |F_{P(obs)}||$ for centric reflections. [f] Phasing power $= [\sum_h |F_{H(calc)}|^2 / \sum_h (|F_{PH(obs)}| - |F_{PH(calc)}|)^2]^{1/2}$ for centric reflections.

the X-ray crystal structure of the heterodimeric luciferase from the bacterium *Vibrio harveyi* at 2.4 Å resolution.

MATERIALS AND METHODS

Crystallization and Data Collection. The genes encoding the alpha and beta subunits of luciferase from *V. harveyi* were expressed in *E. coli*, and the protein was purified as previously described (Baldwin et al., 1989). Crystals were grown by hanging-drop vapor diffusion. Briefly, luciferase (20 mg/mL) was diluted 5 μL:5 μL with reservoir buffer, 1.4 M $(NH_4)_2SO_4$, 200 mM NaH_2PO_4, and 100 mM succinate, pH 5.7, and equilibrated at room temperature. This resulted in larger more reproducible crystals than grown under conditions previously reported (Swanson et al., 1985). Crystals typically grew to the dimensions of 0.6 × 0.4 × 0.3 mm in 3 weeks, after which they were transferred to storage buffer, 2.0 M $(NH_4)_2SO_4$, 200 mM NaH_2PO_4, and 100 mM succinate, pH 6.0. Crystals belong to the orthorhombic space group $P2_12_12_1$ with unit cell dimensions of $a = 59.9$ Å, $b = 112.7$ Å, and $c = 301.8$ Å and diffract X-rays beyond 2.4 Å resolution at a synchrotron radiation source. There are two heterodimers per asymmetric unit ($V_M = 3.2$ Å^3/Da). One native and three derivative data sets were measured to 2.9 Å resolution at 4 °C with a Siemens HI-STAR dual-detector system mounted on a Rigaku rotating anode with focusing mirrors. The crystal to detector distances were 250 and 380 mm and at 2θ angles of −21.0° and 10.8°, giving coverage of the diffraction pattern to 2.7 Å resolution and overlap for scaling between 10.3 and 4.7 Å resolution between the two detectors. Area detector data were processed with the program XDS (Kabsch, 1988) and scaled using the program Xscalibre (G. Wesenberg and I. Rayment, unpublished results). A 2.4 Å resolution native data set was collected from 30 crystals at the Cornell high energy synchrotron source (CHESS)[1] F-1 line on Fuji image plates. The CHESS data were processed and scaled with the programs developed by Rossmann (Rossmann, 1979; Rossmann et al., 1979). Table 1 gives the data collection and heavy atom derivative statistics for structure determination.

Phase Calculation and Refinement. All heavy atom soaks were carried out at room temperature in storage buffer. The heavy atom positions were determined by examination of difference Patterson maps and difference Fourier maps. The heavy atom positions were refined with the program HEAVY (Terwiliger & Eisenberg, 1983) and multiple isomorphous replacement phases computed to 5 Å resolution. The resulting electron density map, when solvent flattened, revealed many continuous segments of electron density that are characteristic of α-helices. The two strongest sites of the platinum derivative mapped to isolated domains of density and were assumed to bind in equivalent positions on each heterodimer. These positions were used as a common origin to compute an electron density real-space rotation function. A maximum correlation of 0.78 was reached after a rotation of polar angles, $\phi = -3.17°$, $\psi = 108.17°$, and $\kappa = 108.26°$, and a molecular envelope was drawn around the averaged map. MIR phases were computed to 2.9 Å resolution, and a new solvent-flatten map was computed. The translation vector and rotation angles were refined, and the density was cyclically averaged. After 20 rounds of averaging the *R*-factor dropped to 22.2% (averaging *R*-factor $= \sum ||F_o| - |F_c|| / \sum |F_o|$, where F_o is observed data and F_c is calculated from the back-transformed averaged electron density map). Several α-helices and β-strands were observed in the subsequent map.

The program FRODO (Jones, 1978) was used to build a polyalanine model for all the β-strands and α-helices of one subunit and many from the other; however, the loops connecting the secondary structural elements were still not detected. Phases computed from the polyalanine partial model were combined with MIR phases, and an electron density map was computed with SIGMAA Fourier coefficients (Read, 1986). After another round of averaging the *R*-Factor dropped to 19.5%. The subsequent electron density map was readily interpretable, and the amino acid sequence could easily be identified, allowing for unambiguous tracing of the peptide chains. Residues 1−271 and 289−355 (of 355) were modeled for the alpha subunit, and residues 1−321 (of 324) were built into the beta subunit. The second dimer in the asymmetric unit was generated by rotation and translation of the first, and the two heterodimers were refined independently by the simulated annealing procedure in X-PLOR (Brünger, 1990) followed by the conventional least squares algorithm in TNT (Tronrud et al., 1987). After five cycles of iterative least squares refinement followed by model rebuilding the *R*-factor decreased to 24.9%. At this time the model was refined against the 2.4 Å resolution CHESS

[1] Abbreviations: rms, root mean square; CHESS, Cornell High Energy Synchrotron Source; MIR, multiple isomorphous replacement; TIM, triose-phosphate isomerase.

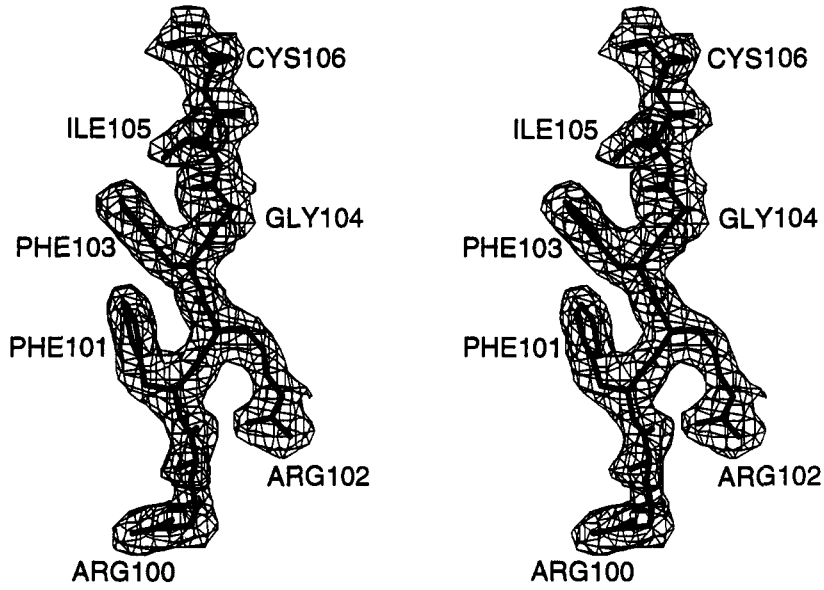

FIGURE 1: Electron density map (stereoview) of β-strand 4 from the alpha subunit. The map was contoured at 1σ and calculated with $2|F_o| - |F_c|$ amplitudes and phases where determined from the final model. The inner core of the β-barrel is to the right of the strand as observed. The figure was drawn with the program MOLVIEW (Smith, 1990).

data. The current *R*-factor for the partially refined structure between the observed and calculated data is 20.8% for all data recorded between 30 and 2.4 Å resolution and includes 10 344 non-hydrogen protein atoms, 201 water molecules, and 2 phosphate ions in the asymmetric unit. The root-mean-square (rms) deviation from ideality for the bond lengths, angles, and trigonal planes is 0.016 Å, 2.71°, and 0.006 Å, respectively. Ninety percent of the non-glycinyl residues reside within the fully allowed region of the Ramachandran plot. The few outliers are located either in flexible loops or at crystal contacts.

RESULTS AND DISCUSSION

Representative electron density for a portion of the alpha subunit is shown in Figure 1. The tertiary structure of both the alpha and beta subunits is very similar. Both subunits fold into a single-domain eight-stranded β/α barrel motif first seen in the crystal structure of triose-phosphate isomerase (TIM) (Banner et al., 1975). The $(\beta/\alpha)_8$ tertiary structure of luciferase was correctly predicted by Moore and James on the basis of the structure of LuxF and its sequence similarity to luciferase and other $(\beta/\alpha)_8$ enzymes (Moore & James, 1994). The two subunits assemble around a parallel four-helix bundle centered on a pseudo 2-fold axis that relates the alpha and beta subunits. Helices α2 and α3 from each subunit form the helical bundle. A 38 Å translation and 80° rotation separate the barrel axis of the alpha subunit from the barrel axis of the beta subunit. The overall dimensions of the luciferase dimer are approximately 75 Å × 45 Å × 40 Å (Figure 2). The core of both β-barrels is mostly hydrophobic. However, the NH_2-terminal core residues are hydrophilic and exposed to solvent. One side of the barrels' COOH-terminal end is hydrophobic and shielded from solvent by an α-helix discussed below.

The topology of the alpha and beta subunits is identical (Figure 3). In both subunits, the most prominent loop of the $(\beta/\alpha)_8$ motif is the one between β7 and α7. This loop is 34 residues long in the beta subunit and contains two α-helices (α7a and α7b) and a short β-strand (β7a). The α7a helix runs along the top of the barrel and bends at residue Leu 247, positioning the last two turns of the helix over the COOH-terminal opening of the barrel. Helix α7b lies on the outside of the subunit and runs antiparallel to helix α7a. Residues Ala 272−Gly 274 form the short β-strand β7a that runs parallel to and hydrogen bonds to the COOH-terminal end of β7.

In the alpha subunit, the β7−α7 loop is 71 residues long and contains the additional 29 residues not present in the beta subunit. The β7−α7 loop of the alpha subunit also contains the only stretch of disordered residues. Amino acids Phe 272−Thr 288 of the alpha subunit are not seen in the electron density map of either dimer in the crystallographic asymmetric unit. In the absence of substrates, these residues are highly sensitive to protease digestion, suggesting that they are part of an accessible or flexible loop (Rausch et al., 1982). However, upon binding $FMNH_2$, this loop is protected from proteolysis, implying that it is involved in flavin binding, and adopts a different conformation (AbouKhair et al., 1985). SDS gel analysis of luciferase crystals indicates that both subunits are intact (data not shown). The disordered region is preceded by a 33 Å long α-helix (α7a) and 14 residues that extend toward the beta subunit. Helix α7a lies across the COOH-terminal end of the barrel and covers approximately half of the barrel opening. The first residue seen after the disordered portion is Asn 289. The segment immediately following the disordered section corresponds to helix α7b of the beta subunit. However, in the alpha subunit, this region adopts an extended conformation originating from the disordered loop. As in the beta subunit, there is a short β-strand β7a that runs parallel to and augments the COOH-terminal end of β7.

All the other β−α loops are short and contain no secondary structural elements except for a short helix (α4a) prior to helix α4 and a hairpin loop after α4. These structural features are conserved between both subunits. The hairpin loop is 19 residues long and runs along one side of the dimer interface. The corresponding pseudo 2-fold related loop runs along the subunit interface on the opposite side. Both loops

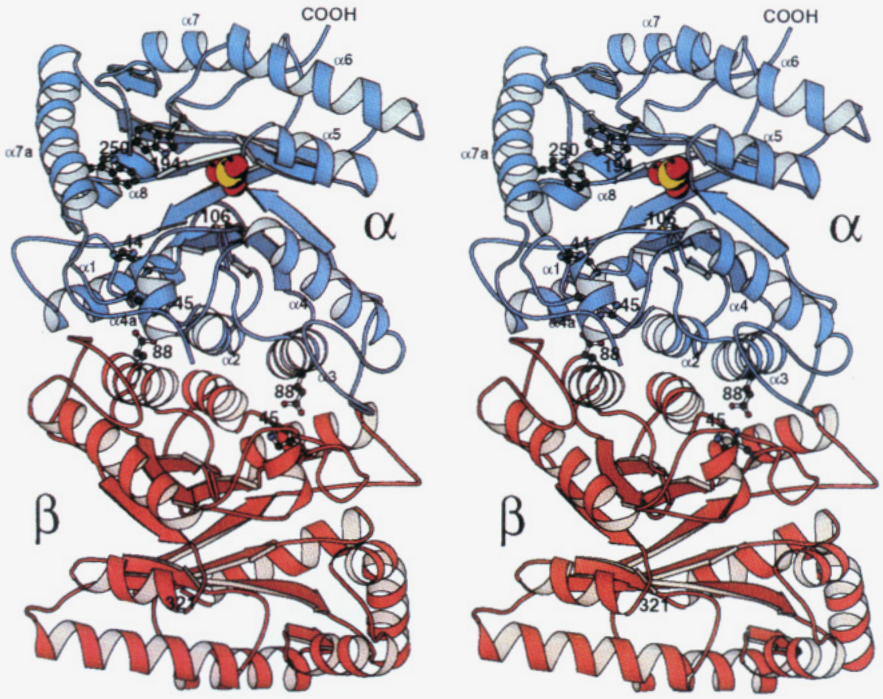

FIGURE 2: Stereo ribbon representation of bacterial luciferase. The view is approximately along the pseudo 2-fold axis that relates the alpha subunit shown in blue to the beta subunit shown in red. The α-helices of the alpha subunit are labeled. The ordered phosphate or sulfate ion is rendered as a space-filling representation. This ion might correspond to the binding site of the phosphate moiety of flavin. Tryptophan residues 194 and 250, which interact with the isoalloxazine ring of flavin, and Cys 106, whose modification hinders flavin binding, are shown as ball-and-stick models. Also rendered as a ball-and-stick model is the conserved intersubunit hydrogen bond between His 45 and Glu 88. This figure and Figure 4 are drawn with the program MOLSCRIPT (Kraulis, 1991).

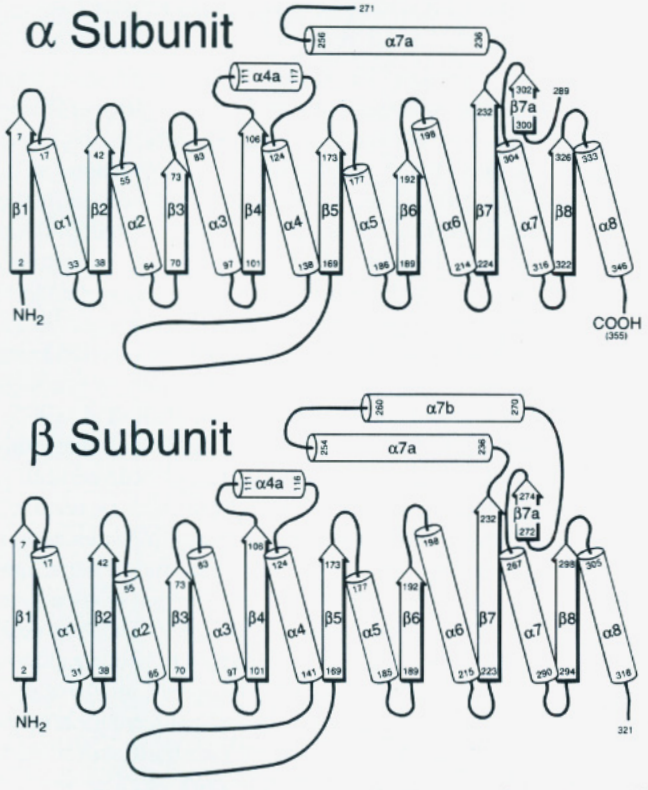

FIGURE 3: Topology diagram showing the secondary structural elements of the two luciferase subunits. β-Strands and α-helices are represented by arrows and cylinders, respectively. The $(\beta/\alpha)_8$ core is drawn flat along the middle with the loop insertions drawn above and below the core. β8 wraps around and hydrogen bonds to β1 to form the closed barrel. The numbers refer to the beginning and end of each secondary structural element.

together embrace the parallel four-helix bundle at the center of the dimer interface. The loops terminate with Pro 160, whose peptide bond adopts the *cis* configuration in both subunits. Pro 160 is conserved among all luciferase alpha and beta subunits.

A total of 2150 Å^2 of accessible surface area is buried upon dimer formation using a search probe radius of 1.4 Å (Lee & Richards, 1971). This value falls in the expected range given the size of the luciferase subunits (Janin et al., 1986). There are extensive interactions between the two subunits across the dimer interface. Most of the intersubunit contacts occur in the parallel four-helix bundle centered around the pseudo 2-fold axis. Helix α2 lies very close to the pseudo 2-fold axis, resulting in a close packing of the α2 helices from each subunit. At one point, the axis of helix α2 in both subunits resides an unusually close 6.6 Å from the pseudo 2-fold related helix axis. In this region, glycines and alanines shape the surface of the helix, allowing for the close contact. In the beta subunit, two leucines from helix α2 interdigitate with a leucine and the aliphatic portion of a glutamate residue to create a leucine zipper interaction with helix α3 of the same subunit. A similar interaction is observed in the alpha subunit except a leucine on α2 is replaced with a phenylalanine and aspartate substitutes for glutamate. The majority of intersubunit contacts established in the four-helix bundle are van der Waals interactions. The hairpin loop structure described above contributes many hydrophobic dimer interactions, which are conserved between the subunits. There are 14 intersubunit hydrogen bonds across the dimer interface. One hydrogen bond of interest occurs between His 45 of the alpha subunit and Glu 88 of the beta subunit. These two residues are conserved among the alpha and beta subunits such that a similar hydrogen bond is also observed between the pseudo 2-fold related residues (beta−His 45 and alpha−Glu 88). Both these residues are conserved among all bacterial luciferase alpha and beta

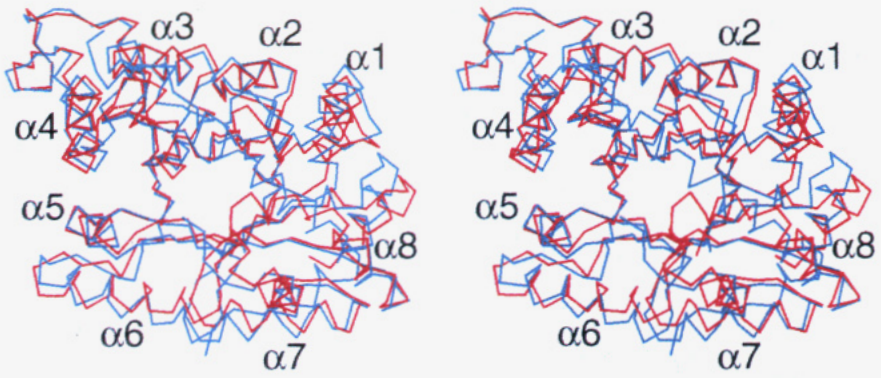

FIGURE 4: α-Carbon stereoview displaying the superposition of the alpha subunit (blue lines) onto the beta subunit (red lines). The perspective is looking down the β-barrel axis with the COOH-terminal end of the barrel pointing out toward the viewer. The eight core α-helices are labeled. The core β-strands superimpose with an rms deviation of 0.62 Å while the entire subunit superimposes with an rms value of 2.6 Å.

subunits, and mutating His 45 in the alpha subunit of *V. harveyi* luciferase results in a substantial decrease of bioluminescence activity (Xin et al., 1991).

There is extensive structural conservation between the alpha and beta subunits corroborating their evolutionary link. The β-barrels from the two subunits superimpose with a rms deviation of 0.62 Å for 42 equivalent α-carbons (Figure 4). The largest deviations between the two subunits are found in helices α1, α4, and α8. These helices are similar in length and composition to their pseudo 2-fold related subunit but are shifted slightly. The region of the beta subunit that contains the 29-residue deletion with respect to the alpha subunit also differs notably in arrangement. In the beta subunit, the last two turns of helix α7a bend to accommodate the shorter connection to helix α7b. In the alpha subunit, helix α7a is straight and extends toward the beta subunit. The regions involved with dimerization, helices α2 and α3 and the hairpin loop structure, are exceptionally similar in the superposition.

All $(\beta/\alpha)_8$ barrel enzymes have active sites at the COOH-terminal end of the β-barrel (Farber & Petsko, 1990). In most cases, the active site is constructed from residues in the loops that connect the β-strand to the subsequent α-helix. The TIM barrel is also a common motif in flavoenzymes (Farber & Petsko, 1990). Glycolate oxidase (Lindqvist, 1989), flavocytochrome b_2 (Xia & Mathews, 1990), trimethylamine dehydrogenase (Lim et al., 1986), and old yellow enzyme (Fox & Karplus, 1994) are all $(\beta/\alpha)_8$ barrels that bind flavin mononucleotide as a coenzyme. These enzymes all share a common structural motif that binds the phosphate moiety of FMN. In this motif, the phosphate ion binds between the β7−α7 loop and the NH_2 terminus of an additional small helix in the β8−α8 loop. This motif is also observed in other TIM barrels that secure phosphate components in their substrates (Wilmanns et al., 1991). Such a motif is not seen in bacterial luciferase. Its absence could explain why luciferase utilizes $FMNH_2$ as a substrate and not as a prosthetic group as in other $(\beta/\alpha)_8$ flavoenzymes. The luciferase electron density map does contain a strong peak of density in the alpha subunit that could accommodate a phosphate or sulfate ion, both of which were present in the crystallization conditions. This position is located between two neighboring loops. The ion hydrogen bonds to the main-chain amide nitrogens of the β5−α5 loop and salt links to the guanido group of Arg 107 in the loop connecting β-strand 4 to helix 4a. Arginine 107 is conserved among all bacterial luciferase alpha subunits. If the phosphate moiety of $FMNH_2$ is anchored at this site, then the flavin can easily be modeled in the COOH-terminal portion of the alpha subunit β-barrel with the isoalloxazine ring situated next to Trp 194 and Trp 250, both of which have been implicated to interact with the flavin ring as measured by fluorescence spectroscopy and circular dichroism spectroscopy (Baldwin and Clark, unpublished results).

In this flavin-bound model, the isoalloxazine ring also lies next to conserved His 44, which is essential for high quantum yield (Xin et al., 1991). Asp 113 of the alpha subunit lies in the α4a helix and points toward His 44. Mutation of this aspartate to an asparagine decreases the binding affinity for reduced flavin by over 450-fold (Baldwin et al., 1987; Cline & Hastings, 1972). Chemical modification demonstrated that the highly reactive thiol from Cys 106 of the alpha subunit lies near the active center, and modification resulted in inactivation of the enzyme (Nicoli & Hastings, 1974; Nicoli et al., 1974). Cysteine 106 is positioned at the end of β4 and points inside the β-barrel. Modification of this thiol would impede $FMNH_2$ binding as modeled.

The organic substrate for bacterial luciferase *in vivo* appears to be myristic aldehyde although aliphatic aldehydes of many lengths can be employed for *in vitro* analysis (Ulitzur & Hastings, 1979). Mutating Ser 227 to larger aromatic side chains such as Phe, Tyr, and Trp decreases the binding for aldehyde by 10-fold but has no effect on flavin binding (Baldwin et al., 1987; Cline & Hastings, 1972). However, changing Ser 227 to the smaller residue alanine has no influence on either flavin or aldehyde binding and displays wild-type activity. Ser 227 is located on β7 and faces the β-barrel interior where it forms the side of a pocket. If this pocket is the long-chain aldehyde binding site, then mutating the pocket's surface residues to fill the space would affect aldehyde binding.

The two subunits of bacterial luciferase are very similar in structure. It is likely that the evolutionary origin of bacterial bioluminescence involved a luciferase homodimer with active sites on both subunits. This is evident from the fact that each separate subunit can generate a very low level of light (Sinclair et al., 1993) and beta subunits can assemble into stable homodimers (Sinclair et al., 1994). Then, through gene duplication, two subunits presumably evolved under selective pressure, resulting in a heterodimer with the highest quantum efficiency. Since the active site is located on the alpha subunit, it appears the beta subunit is required for the

high quantum yield and protein stability. The mechanism of the beta subunit's function is unknown. The additional residues in the alpha subunit lie near the active center and are involved in substrate binding. These residues are part of a disordered loop that is sensitive to proteolysis in the absence of substrates and becomes protected upon binding flavin (AbouKhair et al., 1985; Rausch et al., 1982). Therefore, it appears that the loop forms a lid over the COOH-terminal end of the β-barrel, which closes down on the bound flavin.

This structure determination describes the tertiary structure of a bacterial luciferase and provides a framework for understanding many of the puzzling features of this enzyme. However, in order to establish the molecular basis for the generation of light, it will be necessary to know where and how the substrates bind on the enzyme. These studies are currently in progress.

ACKNOWLEDGMENT

We thank Siemens Industrial Automation, Inc., for kindly loaning the HI-STAR dual area detector.

REFERENCES

AbouKhair, N. K., Ziegler, M. M., & Baldwin, T. O. (1985) *Biochemistry 24*, 3942−3947.

Baldwin, T. O., & Ziegler, M. M. (1992) in *Chemistry and Biochemistry of Flavoenzymes* (Müller, F., Ed.) pp 467−530, CRC Press, Boca Raton, FL.

Baldwin, T. O., Ziegler, M. M., & Powers, D. A. (1979) *Proc. Natl. Acad. Sci. U.S.A. 76*, 4887−4889.

Baldwin, T. O., Chen, L. H., Chlumsky, L. J., Devine, J. H., Johnston, T. C., Lin, J.-W., Sugihara, J., Waddle, J. J., & Ziegler, M. M. (1987) in *Flavins and Flavoproteins* (McCormick, D. B., & Edmondson, D. E., Eds.) pp 621−631, Walter de Gruyter, Berlin.

Baldwin, T. O., Chen, L. H., Chlumsky, L. J., Devine, J. H., & Ziegler, M. M. (1989) *J. Biolumin. Chemilumin. 4*, 40−48.

Baldwin, T. O., Ziegler, M. M., Chaffotte, A. F., & Goldberg, M. E. (1993) *J. Biol. Chem. 268*, 10766−10772.

Banner, D. W., Bloomer, A. C., Petsko, G. A., Phillips, D. C., Pogson, C. I., & Wilson, I. A. (1975) *Nature 255*, 609−614.

Becvar, J. E., & Hastings, J. W. (1975) *Proc. Natl. Acad. Sci. U.S.A. 72*, 3374−3376.

Boyle, R. (1668) *Philos. Trans. R. Soc. London 2*, 581−600.

Brünger, A. T. (1990) *X-PLOR* Yale University, New Haven, CT.

Cline, T. W., & Hastings, J. W. (1972) *Biochemistry 11*, 3359−3370.

Cohn, D. H., Mileham, A. J., Simon, M. I., Nelson, K. H., Rausch, S. K., Bonam, D., & Baldwin, T. O. (1985) *J. Biol. Chem. 260*, 6139−6146.

Farber, G. K., & Petsko, G. A. (1990) *Trends Biochem. Sci. 15*, 228−234.

Fox, K. M., & Karplus, P. A. (1994) *Structure 2*, 1089−1105.

Hastings, J. W., Balny, C., LePeuch, C., & Douzou, P. (1973) *Proc. Natl. Acad. Sci. U.S.A. 70*, 3468−3472.

Janin, J., Miller, S., & Chothia, C. (1986) *J. Mol. Biol. 204*, 155−164.

Johnston, T. C., Thompson, R. B., & Baldwin, T. O. (1986) *J. Biol. Chem. 261*, 4805−4811.

Jones, T. A. (1978) *J. Appl. Crystallogr. 11*, 268−272.

Kabsch, W. (1988) *J. Appl. Crystallogr. 21*, 916−924.

Kraulis, P. J. (1991) *J. Appl. Crystallogr. 24*, 946−950.

Lee, B., & Richards, F. M. (1971) *J. Mol. Biol. 55*, 379−400.

Lim, L. W., Shamala, N., Mathews, F. S., Steenkamp, D. J., Hamlin, R., & Xuong, N. H. (1986) *J. Biol. Chem. 261*, 15140−15146.

Lindqvist, Y. (1989) *J. Mol. Biol. 209*, 151−166.

Meighen, E. A., & Hastings, J. W. (1971) *J. Biol. Chem. 246*, 7666−7674.

Moore, S. A., & James, M. N. G. (1994) *Protein Sci. 3*, 1914−1926.

Nicoli, M. Z., & Hastings, J. W. (1974) *J. Biol. Chem. 249*, 2393−2396.

Nicoli, M. Z., Meighen, E. A., & Hastings, J. W. (1974) *J. Biol. Chem. 249*, 2385−2392.

Rausch, S. K., Dougherty, J. J., & Baldwin, T. O. (1982) in *Flavins and Flavoproteins* (Massey, V., & Williams, C. H., Eds.) pp 375−378, Elsevier, New York.

Read, R. J. (1986) *Acta Crystallogr. A45*, 140−149.

Rossmann, M. G. (1979) *J. Appl. Crystallogr. 12*, 225−238.

Rossmann, M. G., Leslie, A. G. W., Abdel-Meguid, S. S., & Tsukihara, T. (1979) *J. Appl. Crystallogr. 12*, 570−581.

Sinclair, J. F., Waddle, J. J., Waddill, E. F., & Baldwin, T. O. (1993) *Biochemistry 32*, 5036−5044.

Sinclair, J. F., Ziegler, M. M., & Baldwin, T. O. (1994) *Nature Struct. Biol. 1*, 320−326.

Smith, T. J. (1990) *J. Appl. Crystallogr. 23*, 141−142.

Swanson, R., Weaver, L. H., Remington, S. J., Matthews, B. W., & Baldwin, T. O. (1985) *J. Biol. Chem. 260*, 1287−1289.

Terwiliger, T. C., & Eisenberg, D. (1983) *Acta Crystallogr. A39*, 813−817.

Tronrud, D. E., Ten-Eyck, L. F., & Matthews, B. W. (1987) *Acta Crystallogr. A43*, 489−501.

Ulitzur, S., & Hastings, J. W. (1979) *Proc. Natl. Acad. Sci. U.S.A. 76*, 265−267.

Waddle, J., & Baldwin, T. O. (1991) *Biochem. Biophys. Res. Commun. 178*, 1188−1193.

Waddle, J. J., Johnston, T. C., & Baldwin, T. O. (1987) *Biochemistry 26*, 4917−4921.

Wilmanns, M., Hyde, C. C., Davies, D. R., Kirschner, K., & Jansonius, J. N. (1991) *Biochemistry 30*, 9161−9169.

Xia, Z.-X., & Mathews, F. S. (1990) *J. Mol. Biol. 212*, 837−863.

Xin, X., Xi, L., & Tu, S. C. (1991) *Biochemistry 30*, 11255−11262.

BI950561G